Model-Based Design and Characterization
of an Actuator with Low-Boiling Liquid

Christoph Steinmann[1]   Johannes Herold[1]   Jens Schirmer[1]

[1]Institute of Electromechanical and Electronic Design, TUD Dresden University of Technology, Germany
`christoph.steinmann@tu-dresden.de`

Abstract

Visually impaired people rely on special equipment for access to graphic representations in digital form. The available devices are very large and expensive. A simple and cost-effective alternative to the existing concepts for haptic displays is therefore desirable. This paper evaluates the concept of a lifting actuator based on a fluid with a low boiling point for this purpose. A functional prototype is constructed and its behavior is characterized. A corresponding model is built and validated to simulate the actuator and to analyze its operation. It provides detailed information about the actuator that can be used to further develop the design and to make decisions on the usability of the new actuator in the product design process. Following test runs and investigations on the model, the actuator concept proved to be suitable for haptic display devices under certain assumptions. Therefore the newly developed model presents a good starting point for future revisions of the concept.

Keywords: haptic display, multi-domain model, liquid-to-gas phase change actuator, low-boiling liquid

1   INTRODUCTION

Tactile displays make it possible for visually impaired people to interact with graphical representations of information. Text-to-speech or classical braille lines can not fulfill this functionality to the same degree (Baldwin et al. 2017). It is therefore desirable to further improve this type of device.

Information can be made palpable primarily by thermal, electrical or mechanical stimulation. Consequently a variety of actuators can be used to generate these effects. For dot based graphical output the most common method is to feel mechanically elevated surfaces (Vidal-Verdú and Hafez 2007). These can be actuated by electric motors (Wagner, Lederman, and Howe 2002; Sarakoglou, Tsagarakis, and Caldwell 2005), shape memory alloy (Howe, Kontarinis, and Peine 1995; Velazquez et al. 2005), light (Mirvakili et al. 2021), pneumatic devices (Caldwell, Tsagarakis, and Giesler 1999; Wilhelm 2015) or piezoelectric actuators, as often used in commercial products (Tieman and Zeehuisen 1988; Matschulat 2024; Metec AG 2024).

Thermopneumatic actuators are rarely used. They are based on the expansion of fluids due to heat input. When liquids with low boiling points are utilized even more mechanical expansion is obtainable during evaporation. This type of actuator is called a phase change actuator (PCA). A very simple actuator consisting of a closed volume of fluid with the ability to expand directionally can be constructed (Rai-Choudhury 1997; Matsuoka and Suzumori 2014).

This actuator principle could have many advantages because of its very simple structure and the miniaturization potential it offers. The low number of internal components might also lead to a more cost effective design.

There are multiple publications utilizing this principle to generate mechanical force in soft robotics and other fields (Han et al. 2019; Matsuoka, Kanda, et al. 2016; Niiyama, Rus, and Kim 2014; Boyvat, Daniel M. Vogt, and Robert J. Wood 2019; Sanchez et al. 2020; Uramune et al. 2022). Work has also been done on low-boiling liquids in the context of single braille actuators (Vidal-Verdú, Madueno, and Navas 2005) and even on the use of micro electro-mechanical system technology (Kwon, S. W. Lee, and S. S. Lee 2009).

A common shortcoming of existing publications using thermopneumatic actuators for braille displays is the lack of a satisfactory theoretical model to describe the entire system. Available models typically focus only on specific properties or are based on simplified assumptions regarding the thermodynamics of the system. An example of this is the use of the Clausius-Clapeyron equation in (Vidal-Verdú, Madueno, and Navas 2005), which describes the resulting vapor pressure as a function of the temperature. It does not provide any information on the system state and therefore its own validity; nor does it provide any information on transport properties like heat capacity, which is needed to calculate the energy demand. The exact force generated is often characterized by taking measurements on prototypes subsequently.

The goal of this work is to build a useful model of the complete tactile system with standard engineering tools and to make similar models applicable to other designs based on the same principle. For this purpose a thermopneumatic actuator is built based on the braille standard size with a corresponding model describing its behavior. The prototype is then characterized with measurements to validate the model.

2 METHODS

First a basic design is decided upon to then derive a model of the relevant physical effects and the model's theoretical behavior. A demonstrator is constructed on the same basis. Finally, the two are compared by means of experimental validation in order to derive findings for further decisions in the product development process.

2.1 Actuator Design

The actuator meets the requirements of the braille standard, in particular the footprint of 2.5 mm (braille dot size), and represents a single tactile point. The prototype was designed considering the available tools, scalability and general ability to build up a matrix display based on it. This is a more segmented approach comprising discrete components as compared to other more integrated approaches like in Kwon, S. W. Lee, and S. S. Lee (2009). The system comprises only a few components to facilitate modeling (Figure 1 A).

A wide variety of materials with different state transitions (solid to liquid, liquid to gas) can be used to implement the basic principle (Wilhelm, Richter, and Rapp 2018). We decided to use Novec 7000 (also known as HFE 7000 or RE347mcc) because of its low boiling point, good environmental performance and its successful use in other studies by Nakahara et al. (2017), Hiraki et al. (2020), and Narumi et al. (2020).

The working fluid (F) is held in a copper chamber sealed by adhesive copper foil (Figure 1 component "C"). While using this much copper increases the thermal mass and therefore slows down the actuator, it accelerates heat entry and speeds up the process. The latter was the dominant effect with the first prototypes. Thermopneumatic actuators are often designed with thin, flexible membranes primarily made from latex. Tests showed that this is not an option for this prototype using Novec 7000 as a working fluid: The hygroscopic properties of alkoxy perfluoroalkanes (Koenigsegg 2021) might have led to water from the surrounding air migrating through the thin latex layers. Therefore in our design a polyester foil with aluminum coating is used (M). The metal layer makes this seal gastight. The actuator can only expand by curving the foil instead of mechanically stretching it like an elastic membrane. This solution reaches its lower size limit with the design footprint of 2.5 mm but produces a better seal than a latex membrane. The prototype is completed by a small push rod (P) to transmit the force and motion to the touch surface and a spring (S) to assist with restoring the initial position. The actuator itself does not include a heat generating device for the demonstrator. An external Peltier element with temperature control is used to provide the thermal energy needed (H).

### 2.2 Model of the Actuator

Bardaweel et al. (2009) built a detailed model of a PCA by dividing it into discrete elements that are each described by algebraic differential equations. Combining these results in a model describing all relevant internal and external properties of the actuator. This technique of combining differential equations across multiple physical domains in a single system simulation is well suited for thermo-pneumatic actuators. The structure of our chosen design is shown schematically in Figure 2 A. It illustrates that many variables and various physical effects interact with each other in this actuator.

To make a similar approach for our actuator more generally accessible we opted to use the Modelica (Mattsson and Elmqvist 1997) based commercial simulation tool *SimulationX* (*SimulationX* 2024). With this approach a lot of object-oriented basic elements are predefined and easily accessible. A second general advantage of the approach is that the parameters of the idealized individual components can be well estimated in the concept phase and still be easily adjusted later. Hence, models created this way offer a high degree of flexibility. The most important constructive parameters of the prototype are shown in Table 1. These values change when altering the actuator design. Parameters which are constant in this context like material properties are not listed in the table.

In Figure 2 B the network of thermal components in the system is built from the bottom up. It consists of contact resistances between the components and their respective heat capacities. Constructive parameters from Table 1 in this context are contact areas and the mass of the components to calculate heat capacity. The thermal conductivity at the contact points with thermal grease can be determined from the literature (Lienig and Bruemmer 2017). For the heat transfer into the fluid, boiling and condensation processes would theoretically have to be considered, which affect the resistance value depending on the fluid state. Since available models do not properly reflect a wide chamber, like it is used in our design, and since this variable primarily affects system dynamics, the effect is not being modeled more precisely for the time being. It could be integrated in the model in future iterations.
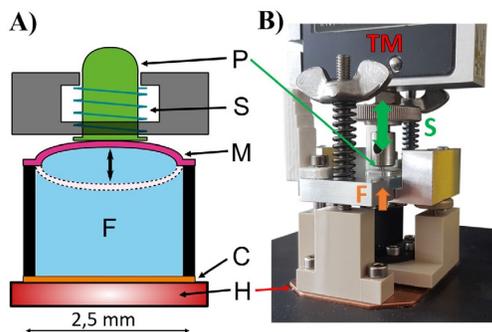
Figure 1. A) Components of actuator prototype from bottom to top: heatplate H, copper foil C, fluid F, membrane/foil M, spring S, pin P
B) Experiment with tensile testing machine TM, stroke S and force F
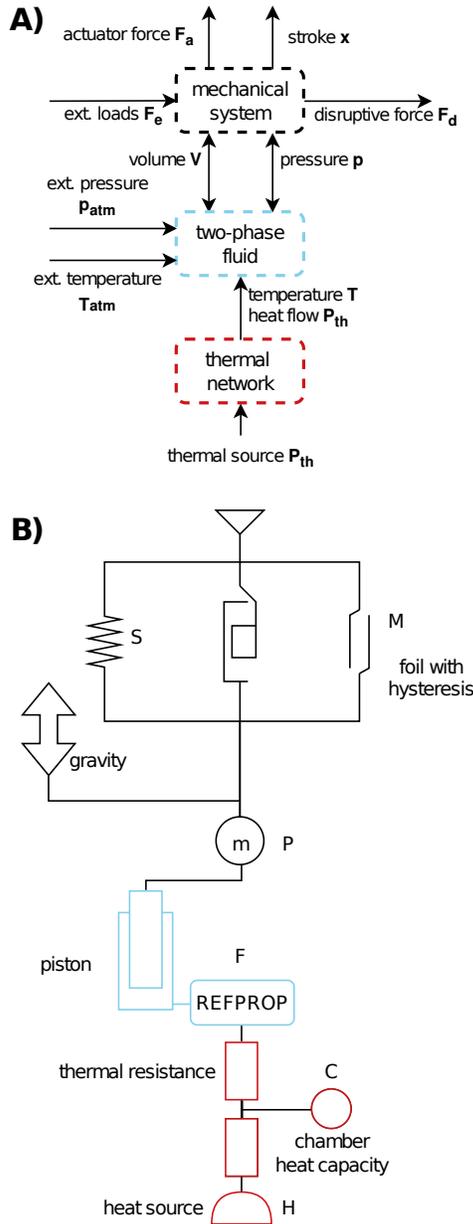
Figure 2. A) Schematic of the different physical domains involved in a PCA and their connections
B) Simplified version of the system model realized with Modelica

The chamber with the working fluid is connected to the thermal network. The thermodynamic properties of the fluid are hard to determine. In principle, the pressure in the fluid can be represented as a function of temperature using the Antoine equation or an empirical function according to the data sheet. With the characteristic points given in the data sheets, the Clausius-Clapeyron equation (Gerlach and Dotzel 2008) describing the vapor pressure can often be evaluated:

$$p(T) = p_k \cdot e^{\frac{L_0}{R}\left(\frac{1}{T_k} - \frac{1}{T}\right)} \qquad (1)$$

Here the critical point tuple (T_k, p_k) and heat of evaporation L_0 can be taken from the manufacturer's data sheet. The universal gas constant R is also well documented. The state of the fluid includes additional variables like the ratio of vapor to liquid phase as well as dependent transport variables, such as thermal conductivity and thermal capacity. In the case of very extensively tested fluids (e.g. water), the corresponding relationships can be found in empirical formulae or tables. But generally such thoroughly verified data is not available for every material.

Table 1. Most important constructive model parameters for nominal (n) and tuned (t) model

component	parameter	value
H,C	radius contact area heater	5.25 mm
H,C	thickness copper bottom	0.05 mm
C	mass fluid chamber	2.1 g
C	radius fluid chamber	1.25 mm
C	volume fluid chamber	23 mm^3
M	movement force foil	36.8 mN
M	stiffness foil (n)	137 N/m
M	*stiffness foil* (t)	*500 N/m*
S	spring constant	585 N/m
P	mass pin	0.5 g
P	maximum stroke	0.6 mm
F	elasticity fluid volume (n)	0.7 mm^3/bar
F	*elasticity fluid volume* (t)	*0.5 mm^3/bar*

Thermodynamic reference models such as CoolProp (Bell et al. 2014), TREND (Span et al. 2020) or REFPROP (Lemmon et al. 2018) offer a solution. Based on the Helmholtz equation of state and appropriate laboratory data, these tools provide both state and transport quantities. They also determine properties that would be unavailable with the above method. REFPROP, which was developed by the National Institute of Standards and Technology (NIST), was used in this work. In order to include the data in the Modelica model, either suitable lookup tables can be generated beforehand and integrated into the corresponding simulation programs or, as in our case, a program interface can be used, which feeds parameters from the current simulation step directly into REFPROP and receives the results. This means that states outside the phase transition region can also be simulated in the fluid section of the model (Figure 2 blue) and energy aspects can be considered by means of the variable material parameters.

The model is completed by the actuator's mechanical components. These consist of basic elements such as springs and masses as well as travel stoppers. Foil behavior (Figure 1 component "M" and Figure 2 B "M") is modeled by a force hysteresis over the deformation path. Hysteresis parameters are obtained from previously performed tests on the physical setup with an external pressure source instead of the fluid. Two parameters in Table 1
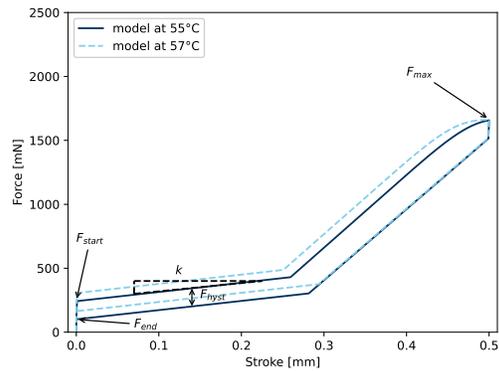
Figure 3. Simulation results with characteristic points on the actuator curve

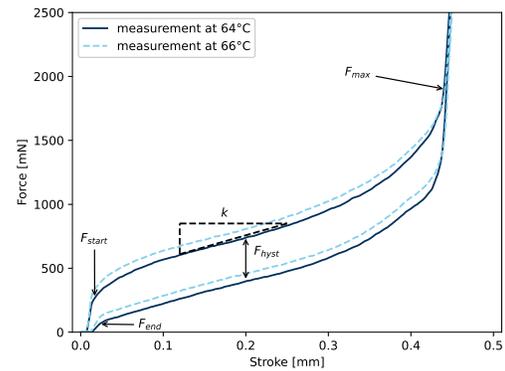**Figure 4.** Test results with characteristic points on the actuator curve

are used to represent the hysteresis in the model: the stiffness of the foil, which determines the increase in force, and a constant force offset, which determines the pressure at which the foil begins to change its direction of movement. The latter was adjusted in a tuned model in section 3. For the purpose of this study, only the observed behavior is used as a basis for modeling. One approach for a more precise modeling would be the phenomenological description of the process using two principles: The stiffness is mainly caused by friction of the foil against itself during flipping. The constant force is comparable to the limit load that leads to plate buckling. However, since the foil represents a design trade off to make the chamber gas tight, a more detailed modeling is not considered to be necessary. Further iterations of the actuator design would need a different solution for this component nonetheless.

2.3 Experimental Validation

The experimental procedure can now be virtually reproduced in the actuator model and the measurable variables can be compared with each other. In addition, the model also provides insight into the system states.

First, the actuator is preheated to a constant temperature and completely extended. In a real-world scenario, a person would now apply a tactile force from above when feeling the actuator. In order to simulate this process and to characterize the actuator as appropriately as possible, the measurement is performed identically: The extended actuator is compressed to the lower end stop by a tensile testing machine (Zwick 1120) and then released. Meanwhile, the force is measured as a function of the actuator stroke. The test cycles are very slow with 40 s for 0.5 mm stroke to enable the readjustment of the temperature, which is assumed to be constant. Each measurement is carried out at least twice on the real prototype. The tests are repeated at different temperatures. A characteristic curve based on the model is plotted in Figure 3.

The plot shows that the force at the beginning (F_{start}) is greater by the amount of the hysteresis force F_{hyst} when moving down than when moving out at the end (F_{end}). As long as steam is still present in the system, the pressure is

constant according to theory, since the temperature is kept constant. The increase k visible in Figure 3 is due to the mechanical properties of the spring and foil.

When leaving the two-phase region, there is a significant increase of up to F_{max} in the force required because the vapor pressure equation loses its validity at this point and the tensile tester is now acting against a noncompressible fluid with no vapor content. This response can only be depicted by using the thermodynamic reference model.

Curves similar to those yielded by the model are also expected in the trials and can be compared based on the characteristic points. Exemplary test results are shown in Figure 4 and variables corresponding to those in the model are plotted for comparison purposes.

3 Results

The experiments show that the fully assembled prototype fulfills the basic function of an actuator for an active braille display. In addition to the functional tests, the test sequence described above was performed 13 times. Figure 4 shows two of these test runs at 64°C and 66°C, respectively.

There is a constant temperature offset of 9 K between the model values and the measurements. This will be discussed later.

3.1 General Behavior

Some basic actuator characteristics were determined prior to the force measurements. It has been shown that the prototype does not start to extend until a temperature of 62°C is reached. The extension and retraction periods of 31 s and 60 s, respectively, are very long with the heating and cooling unit used. The reason for this is that the overall structure is stiffer then it needs to be, which is mainly due to the foil being used to make the system gas tight. The minimum force of 50 mN - required for probing the point (Vidal-Verdú and Hafez 2007) - is greatly exceeded as well. However, these drawbacks are all a direct consequence of the concrete design implementation. With the
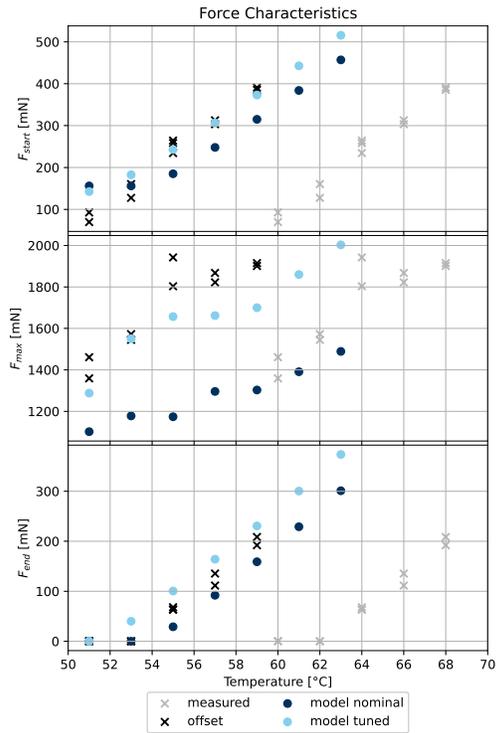
Figure 5. Forces at different temperatures. From top to bottom: force at first contact, maximum force and force after releasing the load

Figure 6. Stiffness (top) and hysteresis (bottom) of the actuator at different temperatures
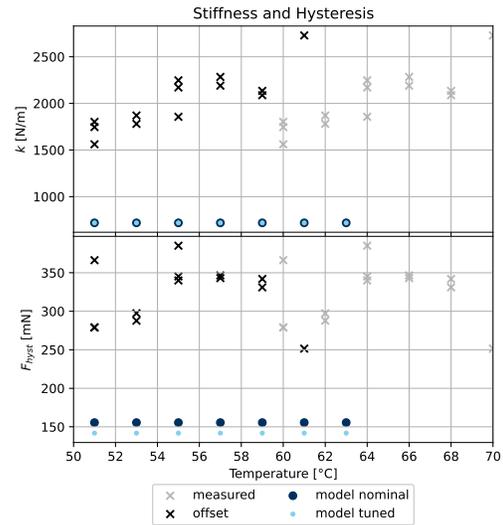
help of the model, it is possible to simulate a smaller actuator with lower heat capacity and less stiff mechanical components that reaches cycle times of 0.1 s with still sufficiently large tactile force.

Although the energy consumption could not be measured in the demonstrator, the results from the model allow conclusions to be drawn in this regard as well. The selected design boundary conditions, such as overall size, mechanical losses and stiffness, are clearly too large. This results in very high energy consumption. In practical terms, this would mean that approximately 1 W of power would be required per actuator in the extreme case of a display with a 10 Hz refresh rate. This is not realistic for applications with several thousand actuators like high resolution tactile displays. The design of the actuator concept would have to be adapted so that it could realistically be operated at lower power levels.

The curve in Figure 4 can be compared with the modeled sequence in Figure 3 and all characteristic values are identifiable for further examination. The plot also shows that the demonstrator does not quite achieve the targeted maximum stroke of 0.5 mm due to mechanical tolerances. Other differences between the curves can be better analyzed using the characteristic points in the next section.

3.2 Actuator Characteristics

The characteristic points in the force-displacement curve are obtained from the experimental procedure described above. This data is used to compare the model and the experiment. In addition to the model with nominal values from the design process, a tuned model was developed, as a result of deviating system parameters (Table 1). In certain areas this new model better corresponds to the measurement. Figure 5 shows the three force points. The force at the beginning of the cycle F_{start} is well reproduced by both models, taking into account the constant temperature offset. The same applies to the force after releasing the load (F_{end}).

The maximum force F_{max} applied during the experiment is significantly less accurate. The parameter for the stiffness of the fluid chamber was changed in the tuned model to achieve a slightly better match. However, this is still significantly less accurate compared to the other two forces. There are two reasons for this: First, the tensile tester compresses the test setup to a defined maximum force, since the stroke could not be used in a control capacity. As a result, the very high peak forces do not originate from the actuator itself but from the mechanical stop between the actuator and the testing equipment. The exact value is therefore difficult to determine from the test data. Secondly, there are also inaccuracies in the model, which compresses a fluid inside a stiff mechanical structure after leaving the two-phase region. This parameter change causes numerical inaccuracies at peak values, which could not be fine-tuned for every test series.

The parameters of the actuator stiffness k and hysteresis width F_{hyst} in Figure 6 can also not be fitted very well and both show a fundamental unsolved problem in our studies: In the demonstrator the actuator stiffness increases with temperature. This behavior is not implemented in the model, since the exact cause of the effect is still unknown. Accordingly, there are strong deviations between model and measurement here.

4 Discussion

In the simulation results (Figure 3), a clear distinction can be made between the two-phase region with steam inside the fluid chamber and the single-phase region with progressive compression. The sharp bend separating the two regions is assumed to occur at a stroke height of around 0.3 mm, however in the test setup it is not nearly as apparent as in the model. It should be noted, that the rightmost part of the curve in Figure 4 results from the actual test setup, in which the actuator is fully compressed and released again. This represents a well repeatable test case, but does not correspond to the practical application. When the elevated surfaces are sensed by touch, the actuator would only be loaded in the left part of the characteristic curve. The relevant characteristic values F_{start} and F_{end} are again well modeled there.

The continuous transition between the two regions in the trial could explain why the stiffness k of the test actuator is higher than in the model. A temperature dependency can be at least partially explained: In the two-phase region, the stiffness depends only on the mechanical components of the system, since the pressure in the actuator remains constant. However, this does not apply to further compression with purely liquid fluid. Changes can occur here since the mechanical properties of the fluid change in relation to temperature. Whether these effects are a sufficiently accurate quantitative explanation for the differences needs further investigation.

4.1 Temperature Offset

The temperature during the experiment was only set on the heater and actively regulated there. It could not be measured inside the actuator itself due to its compact design. It is therefore conceivable that the temperature inside the actuator was slightly lower than inside the heating plate because the device was air cooled. In addition, it was shown earlier that the complete actuator is overall stiffer than the model predicts. This means that the real actuator needs a higher temperature to exert the desired force. Both effects combined can explain the temperature difference between model and experiment.

4.2 Model Inaccuracies

Two simplifications were made in the design of the model. On one hand, the expansion within an ideal cylindrical piston is assumed. In this case, the calculated volume does not exactly match that of the actuator because the foil bulges slightly and does not form perfect edges. On the other hand, the boiling and condensation processes are not accurately modeled. The heat transfer between chamber and fluid is thus only a simplification, which impacts actuator dynamics. However, the impact of both effects on the system should be minimal and does not explain the increase in actuator stiffness as a function of temperature. Enhancing these parts of the model therefore improves the overall model behavior only slightly.

4.3 Future Work

This work shows how a Modelica based simulation model can be used to evaluate an idea during the product development process. Apart from this, the actually implemented structure of the actuator prototype still has room for further improvement that should be addressed in future work. The modeling inaccuracies that occur are mainly related to these components.

The foil used as a membrane was selected to replace latex membranes, which repeatedly showed leaks. The foil for the 2.5 mm diameter prototype actuator is on the limit of usability because of its stiffness. This caused the very high operating temperature and large actuator forces, which are significantly greater than required. A better solution with good sealing properties when used in combination with fluorine-based fluids is needed for future setups.

In addition, the setup should be equipped with more sensors for pressure and temperature monitoring inside the actuator. Even if this means that the targeted size of 2.5 mm is probably not feasible for an experimental setup, this disadvantage is outweighed by the significantly better verifiability of the model.

Furthermore it would be worth considering whether a different fluid could be utilized. The coolant used has a high evaporation enthalpy, due to its intended use for absorbing heat, which is also responsible for the high energy consumption. It might be more advantageous to choose a fluid with a higher boiling point but a lower heat of evaporation. The temperature of the actuator must then be kept close to the boiling point by means of insulation. Unfortunately, substances with similarly low boiling points and at the same time low enthalpy of vaporization, such as isopentane, are often toxic (Chiba and Oshida 1991).

5 Conclusions

It was shown that the system simulation approach in combination with thermodynamic reference models can be used to simulate PCAs for tactile applications. The structure is intuitive due to the existing object-oriented libraries and can be adapted well to further work. They therefore form a useful basis for product development processes when evaluating solution concepts.

A model of an actuator was successfully built and experimentally validated. This makes transient simulations possible. It can be easily adapted to modified designs. The challenges that still exist are largely due to the specific foil used in the actuator.

The model based on Modelica with libraries from *SimulationX* can also be extended to include the previously neglected effects. To do this, it would make sense to first carry out further tests with more measurement options and thus clarify the still unexplained effects in regard to the actuator stiffness. However, due to the energy consumption observed on the model, the actuator concept was not pursued further for the specific planned application of a haptic braille display.

Acknowledgements

References

Baldwin, Mark S. et al. (2017). "The Tangible Desktop". In: *ACM Transactions on Accessible Computing* 10.3, pp. 1–28. DOI: 10.1145/3075222.

Bardaweel, H. K. et al. (2009). "Characterization and modeling of the dynamic behavior of a liquid–vapor phase change actuator". In: *Sensors and Actuators A: Physical* 149.2, pp. 284–291. DOI: 10.1016/j.sna.2008.11.020.

Bell, Ian H. et al. (2014). "Pure and pseudo-pure fluid thermophysical property evaluation and the open-source thermophysical property library CoolProp". In: *Industrial & engineering chemistry research* 53.6, pp. 2498–2508. DOI: 10.1021/ie4033999.

Boyvat, Mustafa, Daniel M. Vogt, and Robert J. Wood (2019). "Ultrastrong and High-Stroke Wireless Soft Actuators through Liquid–Gas Phase Change". In: *Advanced Materials Technologies* 4.2, p. 1800381. DOI: 10.1002/admt.201800381.

Caldwell, D. G., N. Tsagarakis, and C. Giesler (1999). "An integrated tactile/shear feedback array for stimulation of finger mechanoreceptor". In: *Proceedings 1999 IEEE International Conference on Robotics and Automation (Cat. No.99CH36288C)*. Vol. 1, 287–292 vol.1. DOI: 10.1109/ROBOT.1999.769991.

Chiba, S. and S. Oshida (1991). "Metabolism and toxicity of n-pentane and isopentane". In: *Nihon Hoigaku Zasshi - The Japanese Journal of Legal Medicine* 45.2, pp. 128–137. PMID: 1920919.

Gerlach, Gerald and Wolfram Dotzel (2008). *Introduction to microsystem technology: a guide for students*. John Wiley & Sons. Chap. 7.2 Transducers for Sensors and Actuators. ISBN: 9780470058619.

Han, Jie et al. (2019). "Untethered Soft Actuators by Liquid–Vapor Phase Transition: Remote and Programmable Actuation". In: *Advanced Intelligent Systems* 1.8, p. 1900109. DOI: 10.1002/aisy.201900109.

Hiraki, Takefumi et al. (2020). "Laser Pouch Motors: Selective and Wireless Activation of Soft Actuators by Laser-Powered Liquid-to-Gas Phase Change". In: *IEEE Robotics and Automation Letters* 5.3, pp. 4180–4187. DOI: 10.1109/LRA.2020.2982864.

Howe, R. D., D. A. Kontarinis, and W. J. Peine (1995). "Shape memory alloy actuator controller design for tactile displays". In: *Proceedings of 1995 34th IEEE Conference on Decision and Control*. Vol. 4, pp. 3540–3544. DOI: 10.1109/CDC.1995.479133.

Koenigsegg, Christian (2021-10-13). "Liquid heat transfer mixture and use thereof". European pat. EP3757190B1. Alpraaz AB. URL: http://v3.espacenet.com/textdoc?IDX=EP3757190.

Kwon, Hyuk-Jun, Seok Woo Lee, and Seung S. Lee (2009). "Braille dot display module with a PDMS membrane driven by a thermopneumatic actuator". In: *Sensors and Actuators A: Physical* 154.2, pp. 238–246. DOI: 10.1016/j.sna.2008.10.002.

Lemmon, Eric W. et al. (2018). "NIST standard reference database 23: reference fluid thermodynamic and transport properties-REFPROP, Version 10.0, National Institute of Standards and Technology". In: *Standard Reference Data Program, Gaithersburg*.

Lienig, Jens and Hans Bruemmer (2017). *Fundamentals of electronic systems design*. Springer. Chap. 5.4.2 Thermal Interface Materials. ISBN: 9783319558400.

Matschulat, Gunnar (2024). *ABTIM*. URL: http://www.abtim.com/ (visited on 2024-04-26).

Matsuoka, Hiroki, Takefumi Kanda, et al. (2016). "Development of a rubber soft actuator driven with gas/liquid phase change". In: *International Journal of Automation Technology* 10.4, pp. 517–524. DOI: 10.20965/ijat.2016.p0517.

Matsuoka, Hiroki and Koichi Suzumori (2014). "Gas/liquid phase change actuator for use in extreme temperature environments". In: *International Journal of Automation Technology* 8.2, pp. 140–146. DOI: 10.20965/ijat.2014.p0140.

Mattsson, Sven Erik and Hilding Elmqvist (1997). "Modelica - An International Effort to Design the Next Generation Modeling Language". In: *IFAC Proceedings Volumes* 30.4, pp. 151–155. DOI: https://doi.org/10.1016/S1474-6670(17)43628-7.

Metec AG (2024). *Hyperflat*. URL: https://www.metec-ag.de/downloads/hyperflat-flyer-komplett.pdf (visited on 2024-04-26).

Mirvakili, Seyed M. et al. (2021). "Solar-Driven Soft Robots". In: *Advanced Science* 8.8, p. 2004235. DOI: 10.1002/advs.202004235.

Nakahara, Kenichi et al. (2017). "Electric phase-change actuator with inkjet printed flexible circuit for printable and integrated robot prototyping". In: *2017 IEEE International Conference on Robotics and Automation (ICRA)*. IEEE, pp. 1856–1863. DOI: 10.1109/ICRA.2017.7989217.

Narumi, Koya et al. (2020). "Liquid Pouch Motors: Printable Planar Actuators Driven by Liquid-to-Gas Phase Change for Shape-Changing Interfaces". In: *IEEE Robotics and Automation Letters* 5.3, pp. 3915–3922. DOI: 10.1109/LRA.2020.2983681.

Niiyama, Ryuma, Daniela Rus, and Sangbae Kim (2014). "Pouch Motors: Printable/inflatable soft actuators for robotics". In: *2014 IEEE International Conference on Robotics and Automation (ICRA)*. IEEE, pp. 6332–6337. DOI: 10.1109/ICRA.2014.6907793.

Rai-Choudhury, Prosenjit (1997). *Handbook of microlithography, micromachining, and microfabrication: microlithography*. Vol. 39. SPIE press. ISBN: 0-8194-2378-5.

Sanchez, Vanessa et al. (2020). "Smart thermally actuating textiles". In: *Advanced Materials Technologies* 5.8, p. 2000383. DOI: 10.1002/admt.202000383.

Sarakoglou, I., N. Tsagarakis, and D. G. Caldwell (2005). "A portable fingertip tactile feedback array - transmission system reliability and modelling". In: *First Joint Eurohaptics Conference and Symposium on Haptic Interfaces for Virtual Environment and Teleoperator Systems. World Haptics Conference*, pp. 547–548. DOI: 10.1109/WHC.2005.17.

SimulationX (2024). URL: https://www.esi-group.com/products/simulationx (visited on 2024-04-26).

Span, R. et al. (2020). *TREND. Thermodynamic Reference and Engineering Data 5.0*.

Tieman, Frans J. and Kees Zeehuisen (1988-07-19). "Tactile relief display device and method for manufacture it". U.S. pat. 4758165.

Uramune, Ryusei et al. (2022). "HaPouch: A Miniaturized, Soft, and Wearable Haptic Display Device Using a Liquid-to-Gas Phase Change Actuator". In: *IEEE Access* 10, pp. 16830–16842. DOI: 10.1109/ACCESS.2022.3141385.

Velazquez, Ramiro et al. (2005). "A low-cost highly-portable tactile display based on shape memory alloy micro-actuators". In: *IEEE Symposium on Virtual Environments, Human-Computer Interfaces and Measurement Systems, 2005.* IEEE, 6–pp. DOI: 10.1109/VECIMS.2005.1567577.

Vidal-Verdú, Fernando and Moustapha Hafez (2007). "Graphical tactile displays for visually-impaired people". In: *IEEE transactions on neural systems and rehabilitation engineering : a publication of the IEEE Engineering in Medicine and Biology Society* 15. DOI: 10.1109/TNSRE.2007.891375.

Vidal-Verdú, Fernando, Manuel J. Madueno, and Rafael Navas (2005). "Thermopneumatic actuator for tactile displays and smart actuation circuitry". In: *Smart Sensors, Actuators, and MEMS II.* Ed. by Carles Cane, Jung-Chih Chiao, and Fernando Vidal Verdu. SPIE Proceedings. SPIE, pp. 484–492. DOI: 10.1117/12.607603.

Wagner, C. R., S. J. Lederman, and R. D. Howe (2002). "A tactile shape display using RC servomotors". In: *Proceedings 10th Symposium on Haptic Interfaces for Virtual Environment and Teleoperator Systems. HAPTICS 2002*, pp. 354–355. DOI: 10.1109/HAPTIC.2002.998981.

Wilhelm, E. (2015). "Entwicklung eines mikrofluidischen Brailledisplays". PhD thesis. Karlsruhe. ISBN: 978-3-7315-0385-9.

Wilhelm, E., C. Richter, and B. E. Rapp (2018). "Phase change materials in microactuators: Basics, applications and perspectives". In: *Sensors and Actuators A: Physical* 271, pp. 303–347. DOI: 10.1016/j.sna.2018.01.043.